

This item is the archived peer-reviewed author-version of:

Efforts towards an on-target version of the Groebke-Blackburn-Bienaymé (GBB) reaction for discovery of druglike urokinase (uPA) inhibitors

Reference:

Gladysz Rafaela, Vrijdag Johannes, Van Rompaey Dries, Lambeir Anne-Marie, Augustyns Koen, De Winter Hans, van der Veken Pieter.- Efforts towards an on-target version of the Groebke-Blackburn-Bienaymé (GBB) reaction for discovery of druglike urokinase (uPA) inhibitors
Chemistry: a European journal - ISSN 0947-6539 - 25:53(2019), p. 12380-12393
Full text (Publisher's DOI): <https://doi.org/10.1002/CHEM.201901917>
To cite this reference: <https://hdl.handle.net/10067/1606970151162165141>

Efforts towards an on-target version of the Groebke-Blackburn-Bienaymé (GBB) reaction for discovery of druglike urokinase (uPA) inhibitors

Rafaela Gladysz,^[a] Johannes Vrijdag,^[a,b] Dries Van Rompaey,^[a] Anne-Marie Lambeir,^[b] Koen Augustyns,^[a] Hans De Winter,^[a] Pieter Van der Veken^{*[a]}

Abstract: Target-guided synthesis (TGS) has emerged as a promising strategy in drug discovery. While reported examples of TGS generally involve two-component reactions, there is a strong case for developing target-guided versions of three-component reactions (3CRs) because of their potential to deliver highly diversified, druglike molecules. To this end, the Groebke-Blackburn-Bienaymé reaction was selected as model 3CR. We recently reported a series of druglike, urokinase inhibitors serving as reference compounds in this study. Due to the limited number of literature reports on target-guided 3CRs, multiple experimental parameters were optimized here. Most challenging was formation of imine intermediates under near-physiological conditions. The latter was addressed in this study by exploring chemical imine stabilization strategies. Noteworthy, imines are also crucial intermediates of other 3CRs. Such systematic studies are strongly required for further development of the TGS domain, but absent in literature. Hence this work intends to be a reference for future multicomponent-based TGS studies.

Introduction

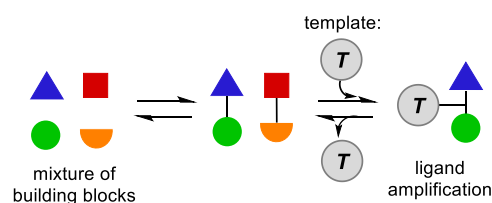
Small molecule drug discovery currently has a wide range of technologies at its disposal for the generation of new “hit” and “lead” compounds. Typically nonetheless, all contemporary strategies revolve around iterative cycles of design, synthesis and potency evaluation, each time producing further optimized compounds. This is a very time-consuming and cost-intensive process, that could be significantly shortened by implementing target-guided synthesis (TGS).^[1]

TGS has emerged as a promising novel strategy to identify ligands for various biological targets.^[1-3] It relies on direct

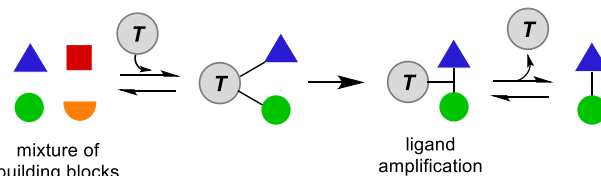
assistance of a drug target, which serves as a physical template that selects ligand building blocks with affinity for the target. Subsequently, the selected building blocks are assembled into finalized ligands based on complementary chemical reactivity and close proximity in the ligand binding site. Building blocks that lack target affinity are not brought to reaction, so that the corresponding ligand constructs are not formed. This effect is known as “selective ligand amplification”. As a consequence, TGS allows combining several aspects of design, synthesis and potency determination, in a single time- and cost-efficient step.

Two main target-assisted strategies have been reported in literature: (1) dynamic combinatorial chemistry (DCC) and (2) kinetic target guided-synthesis (KTGS) (**Figure 1**).^[1-4] DCC uses mixtures of building blocks, which react in a reversible manner. Adding a biological target to this mixture, shifts the thermodynamic equilibrium between the formed products, and in consequence molecules demonstrating the highest target affinity are being amplified “on-target”. Several types of reversible reactions have been used in protein-templated DCC.^[4] However, these reversible reactions often produce metabolically unstable moieties (e.g. imines, hydrazones, disulfides) that are undesirable

(1) DCC: Dynamic Combinatorial Chemistry



(2) Kinetic Ligand Amplification



in drug development, and require isosteric replacement.

Figure 1. Simplified representation of “on-target” approaches in drug discovery.

[a] Dr. R. Gladysz, Dr. J. Vrijdag, Dr. D. Van Rompaey, Prof. Dr. K. Augustyns, Prof. Dr. H. De Winter, Prof. Dr. P. Van der Veken
Laboratory of Medicinal Chemistry (UAMC), Department of Pharmaceutical Sciences
University of Antwerp
Universiteitsplein 1, 2610 Wilrijk (Belgium)
E-mail: pieter.vanderveken@uantwerpen.be

[b] Dr. J. Vrijdag, Prof. Dr. A.-M. Lambeir
Laboratory of Medical Biochemistry, Department of Pharmaceutical Sciences
University of Antwerp
Universiteitsplein 1, 2610 Wilrijk (Belgium)

In the case of KTGS, an approach proposed during the last decade by Sharpless and co-workers, on-target assembly of

ligand molecules proceeds *via* an irreversible step.^[5-7] Here, building blocks showing target affinity, are positioned by the

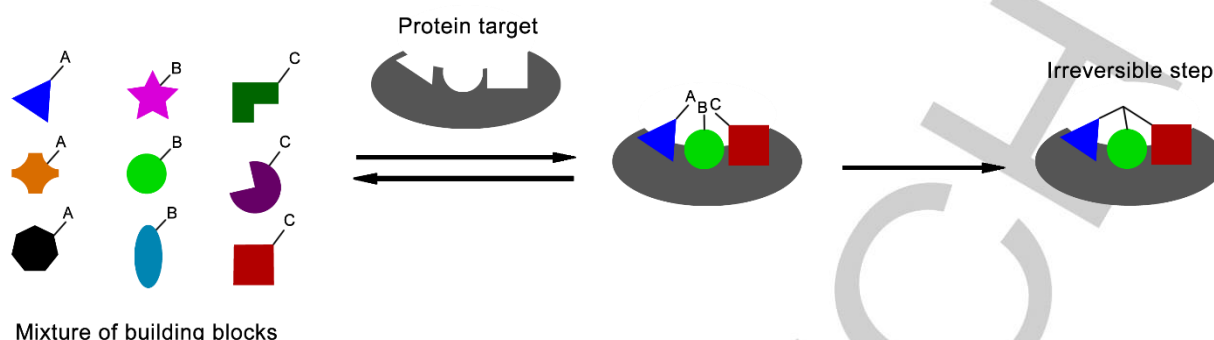


Figure 2. Schematic representation of three-component TGS for enzyme inhibitor discovery.

target in close proximity and correct mutual orientation in order to react irreversibly on-target, affording a new ligand compound. Contrary to DCC, this is a kinetically controlled process, as the biological template brings the reaction partners together, thereby dramatically increasing the reaction rate compared to a non-templated reaction in solution. Hence, amplification and selectivity of ligand formation arise from both target affinity of the building blocks and the target's ability to promote coupling.^[8]

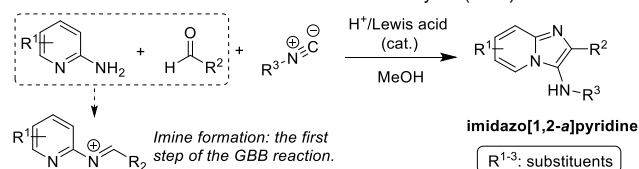
To date, limited but convincing proof for the KTGS methodology has been published. Most examples of this approach rely on a “click reaction”, namely the Huisgen 1,3-dipolar cycloaddition reaction.^[7,9,10] The latter possesses several features which make it well-suited for on-target development, including bioorthogonality, selectivity, and compatibility with aqueous media. Other reports of KTGS involve the sulfo-click reaction,^[11,12] amidation,^[13] alkylation of nucleophiles with alkyl halides^[14] or epoxides^[15], as well as nucleophilic conjugate addition^[16,17]. In terms of biological targets, KTGS has been applied to a number of medically relevant enzymes that mainly belong to the class of hydrolases, e.g., HIV-protease^[6], Factor Xa^[13], insulin-degrading enzyme (IDE)^[10] and acetylcholinesterase (AChE)^[7,9,17,18]. In addition, KTGS has been used for inhibitor development for kinases^[16], carbonic anhydrase-II (CA-II)^[14,19] and biotin protein ligase (BPL)^[20]. Interestingly, at least two molecules obtained by KTGS were employed in *in vivo* research: (1) an inhibitor of CA-II served as the basis for a PET-imaging probe, while (2) a catalytic-site inhibitor of IDE (BDM44768) was evaluated for *in vivo* pharmacokinetics and pharmacodynamics.^[10,21]

In order to increase the practical value of target-guided approaches for drug discovery, further methodological innovation is strongly required. A main attention point is the identification and elaboration of chemical reaction types that are amenable to on-target approaches. Special attention in this framework should be given to reaction types that are capable of deliver “druglike” molecules and have a wide functional group compatibility in order to allow diversity-oriented synthesis. With this respect, multicomponent reactions (MCRs) that are widely used in classical combinatorial drug discovery seem particularly interesting (**Figure 2**).^[22] So far, however, this area remains

largely unexplored: published examples mostly rely on two-component reactions, and only two examples of a target-guided MCR appeared in literature. The first example was mentioned in a review article by Weber,^[23] and entails the application of an Ugi-type reaction in the target-guided identification of a thrombin inhibitor. It is remarkable however that to date no original report on this work has appeared, rendering a detailed assessment of this achievement impossible. The second, and most recent example reported by Rademann and co-workers, describes a target-assisted Mannich-3CR of STAT5 inhibitors involving an aromatic amine, formaldehyde and several N-heterocycles.^[24]

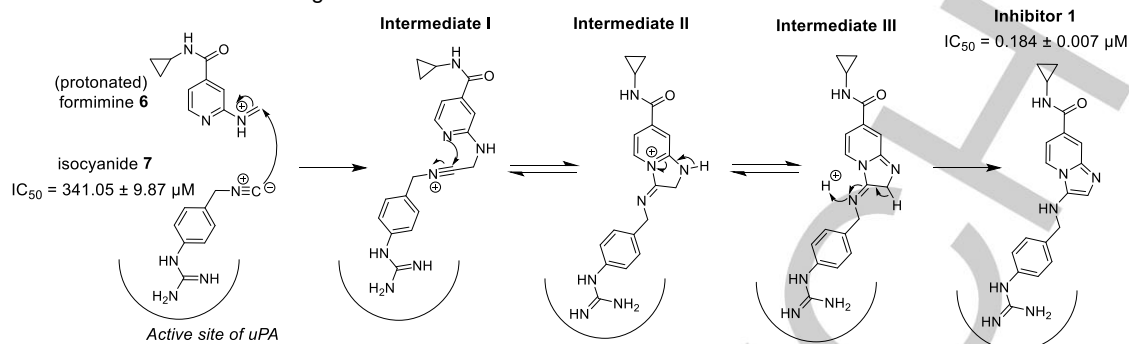
In response to the limited number of reports on target-assisted MCRs, we decided to focus on development of a TGS application of the Groebke-Blackburn-Bienaymé (GBB) condensation, an isocyanide-based three-component reaction with high interest to drug discovery. It features an aminopyridine, aldehyde, and isocyanide building block that react to afford a fused imidazo[1,2-*a*]pyridine (**Scheme 1**), equipped with substituents that allow structural diversification. Imidazopyridines and related heterobicyclics are frequently encountered scaffolds in drug discovery. In this framework, the potential of the GBB condensation to deliver compounds with a highly druglike, “decorated scaffold” architecture is a particular characteristic that sets it apart from several other isocyanide-based 3CRs.^[25] The GBB reaction proceeds *via* two key steps: (1) a reversible reaction between the 2-aminopyridine component and aldehyde forming a Schiff base (imine), and (2) an irreversible step involving a non-concerted (4+1) cycloaddition between the protonated Schiff base and isocyanide, finally followed by a 1,3-H shift.^[26-28]

Scheme 1. The classical Groebke-Blackburn-Bienaymé (GBB) reaction.



With this work, we wanted to address two main research questions. First of all, we wanted to investigate whether the GBB transformation is chemically and methodologically compatible

with typical TGS conditions (involving near-physiological aqueous conditions and low concentrations of reagents and



Scheme 2. Intermediate structures of the GBB reaction docked in the active site of uPA.

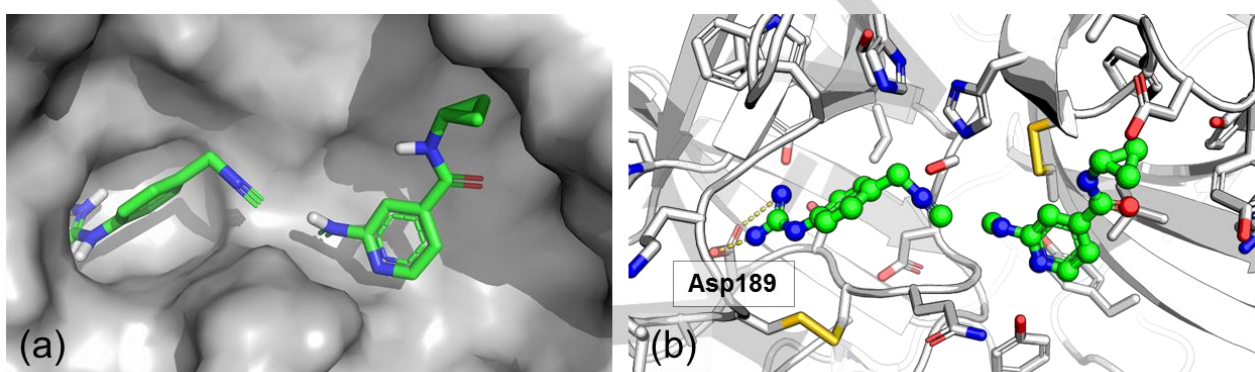


Figure 4. The proposed binding mode of reactants: isocyanide **7** and formimine **6**, in the uPA active site (PDB code 4MNW)^[33-35] in the (a) surface, (b) sticks representation. Putative hydrogen bonds are shown as dashed yellow lines.

protein template). Second, we aimed to demonstrate that “selective ligand amplification” involving the GBB-3CR can be achieved under TGS conditions. We envisioned that this work could be a reference for future KGTS-studies focusing on MCRs. To obtain maximally reliable and verifiable results, we decided to rely on a well-defined model system, involving urokinase plasminogen activator (uPA) as the target protein. Urokinase is a trypsin-like serine protease, and a valuable oncology target that

is overexpressed in metastasizing solid tumors.^[29-31] A set of potent imidazopyridine-based inhibitors of uPA **1-2**, together with a number of less potent analogues **3-5**, served as reference compounds in this study (**Figure 3**). The synthesis of these molecules (*via* classical, solution phase GBB reaction), and their uPA potencies were reported previously by us.^[32]

To the best of our knowledge, the presence of such a well-defined experimental framework is rather unique in TGS. Nonetheless, at this early stage of research we deemed it necessary to pursue reliable step-by-step exploration and optimization of experimental parameters.

Results and Discussion

Before proceeding with TGS of uPA inhibitors *via* the GBB reaction, we decided to investigate the feasibility of the approach by means of molecular modeling. A docking study was pursued by the different reaction intermediates leading to inhibitor **1**, starting from the irreversible step of the GBB reaction: the addition of an isocyanide to an iminium function. Further steps of the reaction comprise conformational rearrangement, ring closure and tautomerization (**Scheme 2**).^[25-28] With this respect, the formimine **6** and isocyanide **7** were selected and the binding mode of the two intermediates in uPA was assessed.^[33-35] Relative binding

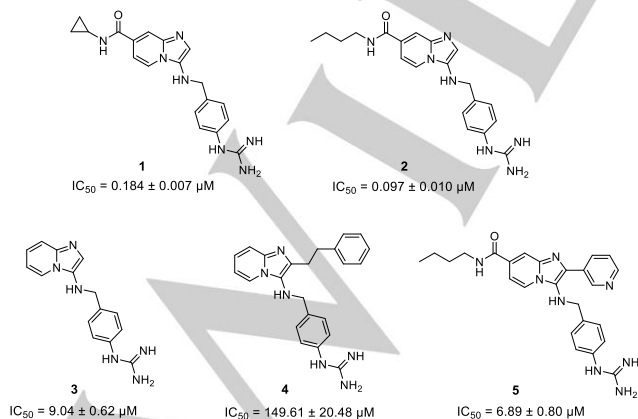
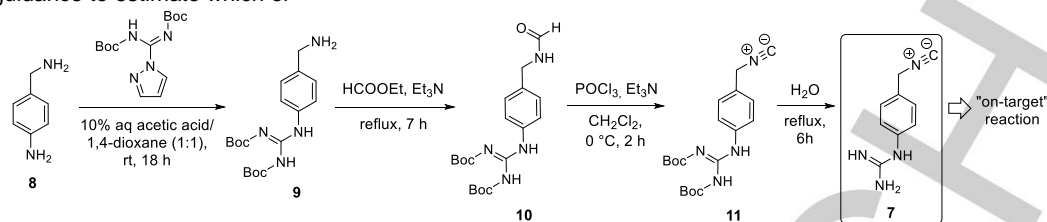


Figure 3. Structures and inhibitory activities of imidazopyridine uPA inhibitors **1-5** used as references in this study.^[32]

affinities (see Supporting Information, Figure S3b, Table S1) were used as a guidance to estimate which of



Scheme 3. Synthesis of the isocyanide building block for the on-target GBB reaction.

the two intermediates is binding as the first one. The phenylguanidine-moiety of **7** was found to bind uPA's S1-pocket, engaging in a salt bridge with Asp189, while the isonitrile group of **7** extends into the solvent-exposed part of the active site. Formimine **6** was subsequently docked into the [uPA-**7**] complex, treating **7** as a part of the receptor. As shown in **Figure 4**, reactant **6** is predicted to bind near reactant **7**, with a distance between the imine carbon and the isonitrile carbon of 3.6 Å. The reactants can thus pre-coordinate in the protein cavity in a conformation favourable for the GBB reaction to occur.

The subsequent intermediates and final compound **1** were then docked (displayed in **Figure 5**). The latter revealed that all intermediates could bind the target in a way that is largely comparable to the binding mode of inhibitor **1**, and that conformational changes between the intermediates were compatible with steric constraints in uPA's active centre. In conclusion, these results indicate that uPA may be amenable to on-target synthesis using the GBB reaction.

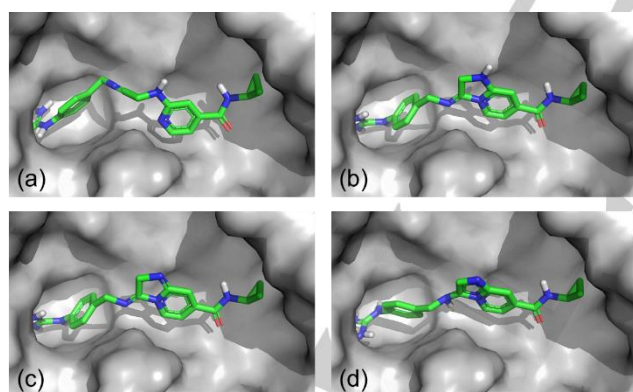


Figure 5. The proposed binding mode of the GBB reaction intermediate structures: (a) intermediate I, (b) intermediate II, (c) intermediate III, and (d) the final compound **1** in the uPA binding site (PDB code 4MNW).^[33-35]

Next, we also considered the possibility of covalent modification of the enzyme by the reaction partners (2-aminopyridine, aldehyde, isocyanide) based on the literature. Regarding the 2-aminopyridine reaction partner, we do not expect any relevant modification of the enzyme. The aldehyde reaction component is slightly more prone to modify the enzyme by, for

instance, reacting with lysine side chains, forming imines. This is, however, a reversible reaction. Nonetheless, aldehydes are known to also participate in N-terminal modifications of proteins, that are not reversible under the conditions of the experiment.^[36] This N-terminal modification, however, is not affecting the enzyme's active site. Moreover, aldehydes have been widely used in target-assisted approaches.^[4,24] Taking into account the presence of aldehydes in living cells, and the aforementioned arguments, in our opinion, the use of an aldehyde reagent should not interfere in our on-target experiments. Regarding the isocyanide reaction component, the reagents of this class are used in bioorthogonal click chemistry. An example thereof was reported by Stöckmann and co-workers, and it presents a bioorthogonal ligation of isocyanides and tetrazines.^[37]

Synthesis

Prior to the actual TGS experiments, appropriate building blocks were synthesized. The most challenging was the preparation of isocyanide **7** (**Scheme 3**). To the best of our knowledge, this is the first reported compound that contains both an isocyanide and a free guanidine moiety. We envisioned that the Boc-protected analogue **11** that we reported earlier, would be a suitable synthetic precursor. In line with earlier reports however, we found that application of acidolytic protocols for Boc-removal, under all evaluated conditions caused instability of the isocyanide function. Surprisingly, we found that refluxing the Boc-protected precursor **11** in water under neutral conditions, allowed to obtain the desired isocyanide **7** in high yield and without the need for further purification. Noteworthy, in aqueous acidic media isocyanides tend to hydrolyse fast to their corresponding formamides.^[38] The other building blocks required for the GBB reaction (aldehydes and aminopyridines) were either obtained from commercial suppliers or prepared using previously reported procedures.^[32]

TGS protocol optimization

In subsequent steps, we aimed at developing a general on-target protocol for the GBB reaction. Herein, specific open questions were related to (1) the nature/composition of the reaction medium, (2) the use of stoichiometric vs. non-stoichiometric concentrations of reactants and enzyme and (3) the LC-MS methodology for analyzing the reaction mixtures. Finally, (4) the lower limits for reagent concentrations were investigated. Because attempts to

FULL PAPER

express uPA in *E. coli* did not produce sufficient amounts of the enzyme, medical uPA (trade name: Actosolv) was used in this study.^[39] The latter is a registered thrombolytic used in hospitals. While protein purity of medical uPA is > 99%, the enzyme is formulated with protein-stabilizing additives. Removal of the latter using a desalting column proved to be crucial for the on-target experiments. Overall, this is a potentially relevant attention point in all TGS studies, because many protein stabilizers, even in trace amounts, might interfere with the on-target experiments.

Reaction medium

First, an appropriate reaction medium for the target-guided GBB reaction was identified. In general, protein-templated reactions are carried out in aqueous buffer solutions at physiological pH or at the target's pH optimum. Both aqueous conditions and appropriate pH range ensure that the target protein is present in a correctly folded conformation: the latter is a strict prerequisite for templated synthesis. Incompatibility of the GBB reaction with aqueous conditions was not expected because the mechanistically related Ugi- and Passerini-type transformations have been reported to run in water.^[40-42] Finding appropriate pH conditions however was anticipated to be particularly challenging, mainly because the GBB condensation involves imine formation as its first and rate-determining step, a characteristic it shares with many other types of multicomponent reactions. Imine formation is known to be an acid-catalyzed process with highest rates at pH 4-6, while uPA's pH optimum is close to 8.5.^[43] Therefore, a compromise had to be found that allowed for the GBB reaction to proceed at acceptable rates at relatively low reagent concentrations, while uPA remains correctly folded. As a proxy for correct protein folding, we measured enzymatic activity: this implies the presence of a properly folded protein. Noteworthy, several other factors than protein folding can affect enzyme activity as well, for example the pH-dependent protonation state of catalytically active residues. Absence or decrease of activity therefore not necessarily means that the protein is denatured.

Furthermore, many classical buffers used in enzymology or in protein formulation contain functional groups that can interfere with the desired GBB reaction and could lead to formation of Ugi or Passerini-type side products. Two examples thereof were encountered during this study. First, products of a Passerini-type condensation between isocyanide **7**, aldehyde, and glycine were unexpectedly identified in on-target reaction mixtures. These were traced back to glycine used as a stabilizer in the 'medical' uPA formulation. Second, a Passerini-type reaction was found to occur between isocyanide **7**, aldehyde and water, in specific reactions where phosphate ions were present in the buffer mixture. Indeed, phosphates are known catalysts of several reactions,^[44-46] and this should be considered while designing on-target experiments. More information on the Passerini-type side reactions observed in this study can be found in the Supporting Information (Schemes S6 and S21-S22, Figures S9-S10, Table S2).

Based on these considerations, two structurally related buffers were selected: (1) HEPES (pKa₂(20 °C)= 7.55) for experiments at pH 8.0 and pH 7.0 and (2) MES (pKa(20 °C)=

6.15) for experiments at pH 5.5.^[47] Both of the selected buffers are compatible with uPA's catalytic activity and lack functional groups that can participate in isocyanide-based 3CRs reaction.

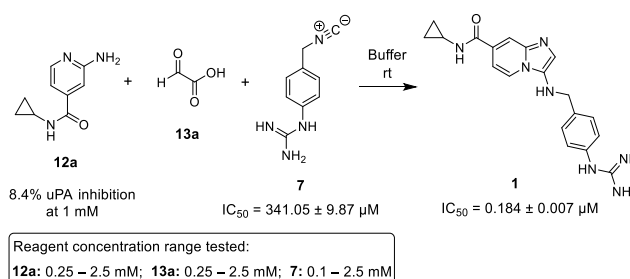
TGS experiments are commonly performed at relatively high enzyme concentrations (i.e., in the micromolar range).^[1] Since most enzymes contain multiple ionizable amino acid side chains, they can affect the pH of the medium. With an isoelectric point (pI) of 8.69,^[48] uPA has the potential to basify the reaction medium if insufficiently buffered. In this study, a 0.2 M buffer concentration was needed to exclude a direct influence on pH by the enzyme.

In order to ensure sufficient solubility for a wide range of organic building blocks employed in TGS experiments, the influence of co-solvents was investigated. To this aim, the enzymatic activity was evaluated in the presence of varying concentrations of three typical organic co-solvents: methanol, dimethyl sulfoxide (DMSO), and acetonitrile (see Supporting Information, Figure S1). Based on the obtained results, DMSO was selected as the most optimal co-solvent. The latter did not cause appreciable loss of uPA's activity when used at 5% v/v. Additionally, DMSO's generally known biocompatibility makes it one of the most commonly used organic solvent in biochemical assays.^[49] The lifetime of uPA was monitored in the selected buffer media, and was proven satisfactory (see Supporting Information, Figure S2).

Reactant Concentration

In general, reported examples of KTGS employ micromolar up to low-millimolar reactant concentrations in order to allow robust analysis of the formed ligation product. Both stoichiometric and non-stoichiometric combinations of building blocks have been reported.^[1,13] In case of non-stoichiometric variants, the building block which is expected to possess the highest affinity has usually been the concentration-limiting reagent. Nonetheless, an experimentally backed discussion on the rationale behind the selection of a stoichiometric or non-stoichiometric experimental set-up is virtually absent in literature.

In preliminary experiments, the rate of the GBB reaction was first determined in the selected buffers in the absence of enzyme. As a model, the GBB condensation of 2-aminopyridine **12a**, glyoxylic acid **13a**, and isocyanide **7** was taken, affording one of the most potent uPA inhibitors within the reference set: compound **1** (IC₅₀ = 0.184 ± 0.007 μM) (**Scheme 4**). Glyoxylic acid was used here as an efficient formaldehyde equivalent.^[32] Mechanistically, spontaneous decarboxylation is known to occur as the last step of the GBB reaction using glyoxylic acid.



Scheme 4. The GBB reaction for the formation of uPA inhibitor 1.

Here, stoichiometric reactant concentrations in the sub-millimolar to low millimolar range were compared with non-stoichiometric variants (**Scheme 4**). In HEPES buffer at pH 8.0 (the 'classical' uPA assay buffer), the rate of the GBB reaction was neglectable in all cases. Not unexpectedly, HEPES buffer at pH 7.0, which is still close to the optimal pH of the enzyme, increased the reaction rate when compared to the initial conditions. In the latter case, the GBB reaction using all the reagents at 2.5 mM concentration afforded 1.1 μM of product **1** after 24 h (0.044% yield). In MES buffer at pH 5.5, although further from the uPA optimal pH, a further increase in the 3CR rate was observed compared to the reaction at pH 7.0. In this case, the same reaction afforded 5.2 μM of product **1** after 24 h (0.21% yield). Although product formation rates at pH 7.0 and 5.5 were still low in absolute terms, this was not considered problematic for the TGS-approach, taking into account that a uPA-promoted process could be considerably faster. Furthermore, we hypothesized imine-formation to be critically implicated in the observed low product formation rates. Chemical imine stabilization strategies (*vide infra*) therefore were expected to further amend this situation. Based on all these data, two standardized experimental conditions were defined for use in the subsequent TGS experiments. The first (referred to as **conditions A**) uses GBB-reactants at 1 mM concentration in MES buffer / DMSO (95:5) at pH 5.5. The second (referred to as **conditions B**) involves GBB reactants at 2.5 mM in HEPES buffer / DMSO (95:5) at pH 7.0. The higher reactant concentration in the latter was chosen to compensate for the intrinsically lower reactivity at pH 7.0.

Next, the concentration of uPA for use in the TGS experiments, was studied using the same model reaction towards inhibitor **1** (**Scheme 4**). A recent review claims that in TGS experiments, the target should ideally be present in a similar concentration range as the reactants.^[1] Multiple literature examples have nonetheless demonstrated ligand amplification with a catalytic amount of the biological target.^[10,13,20,50] In response to this divergence, three possible experimental set-ups were investigated: (a) catalytic enzyme concentrations (0.5 – 2 mol%), (b) enzyme concentrations comparable to the building block concentration, and (c) enzyme concentrations higher than the building block concentration. The two latter scenarios were found not to be favorable. Experiments involving high concentrations of uPA showed substantially lower product formation rates than negative controls in buffer. As a result, the final on-target experiments were performed in the presence of a catalytic amount (approx. 1 – 2 mol%) of uPA. A summary of all experimental conditions determined so far is given in **Table 1**. Noteworthy, the preliminary experiments involving uPA were not indicative of ligand amplification. Due to the early stage of the study however, no conclusions were drawn at this point.

Analytics

To date, most of the reported examples of TGS, use LC-MS in the Selected Ion Monitoring (SIM) mode as analytical methodology.^[1, 51] Although highly sensitive, SIM is not a method that by default allows quantitative analysis.^[1] To the best of our

Table 1. Optimized experimental parameters for TGS of uPA inhibitors.

Parameter	Optimized conditions for TGS
1. Reaction medium	
a. Buffer, pH	MES buffer of pH 5.5 (conditions A) HEPES buffer of pH 7.0 (conditions B)
b. Buffer molarity	0.2 M
c. DMSO content	5% v/v
2. Reagent concentration	Stoichiometric, 1 mM (conditions A) Stoichiometric, 2.5 mM (conditions B)
3. Enzyme ^[a] concentration	Catalytic, approx. 21 μM , corresponding to approx. 1 mol% (cond. B) or 2 mol% (cond. A)
4. Reaction time	24 h - 48 h

[a] Target enzyme, urokinase plasminogen activator,^[39] was purified before on-target experiments using a desalting column, and the protein concentration was determined spectrophotometrically according to the equation: $[\text{uPA}] = \text{OD}_{280} / \epsilon_{(\text{uPA})}$; where OD_{280} - absorbance at $\lambda = 280 \text{ nm}$, ϵ - absorbance coefficient, for mature human urokinase it equals 1.527.^[48]

knowledge, existing LC-MS-SIM-based TGS reports therefore do not provide reliable quantitative data. Nonetheless, Manetsch and co-workers^[18] were able to determine a range in which the SIM-peak areas linearly correlated with compound concentrations. Alternatively, Tieu and co-workers performed product quantitation separately by comparing compound peak area in the UV trace to a standard curve obtained using the reference compound.^[20] It also deserves mentioning that reference compounds are also used in many other TGS-studies, but they rather serve to confirm the identity of the formed products (in terms of m/z , t_r), than for quantitative calibration of the SIM-methodology.^[6, 10-11, 52] Moreover, Rademann and co-workers have applied high-resolution HPLC-QTOF-MS (QTOF: quadrupole-time-of-flight) in KTGS studies.^[13, 24] In these reports, the obtained ligation products were quantified based on calibration curves determined with reference molecules. Importantly, in one of these reports, also the rate of product formation was determined.^[13]

Also tandem mass spectrometry (MS/MS), by involving several steps of ion fragmentation and selection, allows for thorough quantitative analysis of reaction mixtures. Since we considered quantitative analysis an absolute prerequisite for correct interpretation of the TGS data, we relied on a UPLC-TQD-MS instrument (TQD: tandem quadrupole detector) in the Multiple Reaction Monitoring (MRM) mode. The latter allows to monitor

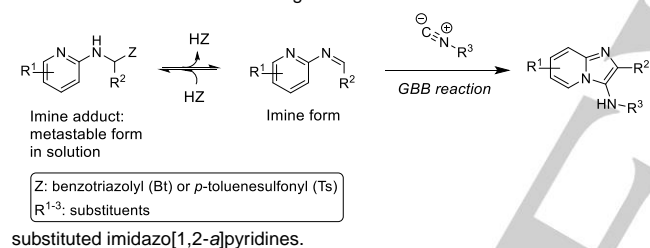
FULL PAPER

product ions based on the formed parent-daughter ion couples, known also as transition couples.^[53-54] This feature reduces the risk of false positive results. Additionally, MRM-MS records the intensity of the detected transition couples, which is proportional to the actual ligand concentration. Hence, MRM enables both qualitative and quantitative analysis of the detected hit compounds. The MRM method is created using reference compounds. In this study, for each of the investigated compounds **1-5**, a separate MRM method was prepared, and the product quantification was based on calibration curves (see Supporting Information, Figures S4-S8).

Imine stabilization

Next, effort was put in addressing the problem of the sluggish imine formation in aqueous media and at suboptimal pH. Hence, we evaluated the possibility of chemically stabilizing preformed imine intermediate in the form of a reversible adduct with (1) benzotriazole or (2) *p*-toluenesulfinic acid. This strategy allows for a quantitative pre-condensation of amine and aldehyde building blocks. Furthermore, the reversible nature of adduct formation, also ensures that the imines are released again over time by the adducts, making them available for reaction with the isocyanide *via* a pseudo two-component reaction (2CR) (**Scheme 5**).

Scheme 5. Pseudo 2CR using stabilized imine intermediates towards

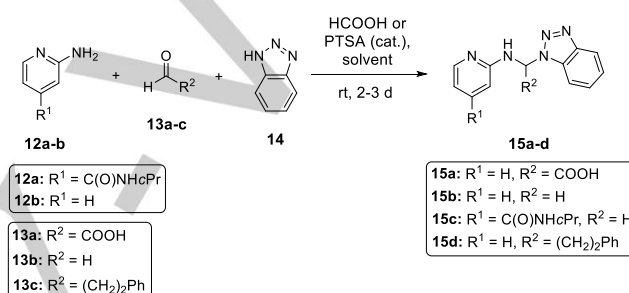


Benzotriazole adducts of imines and related functionalities have been studied most extensively by Katritzky and co-workers.^[55-58] Such adducts have been used in, among others, the Strecker reaction^[55], and the alkylation of (hetero)aromatic systems.^[59] Interestingly, this strategy has also been reported for the synthesis of functionalized imidazo[1,2-*a*]pyridines.^[60-61] Although involving the GBB reaction, the latter examples differ from the strategy applied here by requiring an intermediate methylation step, and a metal catalyst. Likewise, the *p*-toluenesulfinic acid adducts of imines have been reported for the Strecker reaction,^[62-63] and for the solid phase synthesis of dihydropyrimidinones.^[64]

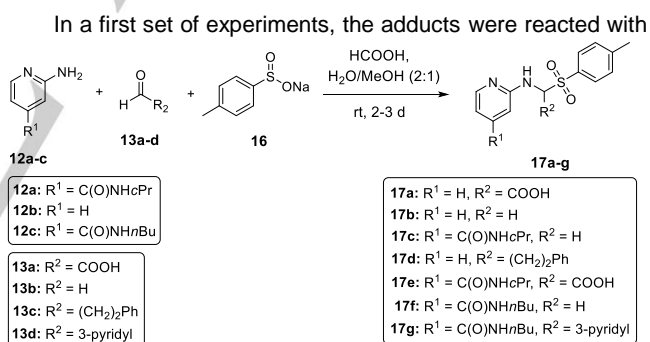
In total, four benzotriazole- and seven *p*-toluenesulfinic acid adducts were synthesized in this study (**Scheme 6** and **Scheme 7**, respectively). Upon reaction with isocyanide **7**, all of these produce one of the reference inhibitors **1-5**. Next to phenylpropanal and 3-pyridinecarboxaldehyde, both formaldehyde and its equivalent glyoxylate were used as the aldehyde building blocks in the adducts. Because the -COOH group in the latter is known to spontaneously decarboxylate after the GBB condensation (*vide supra*) we wanted to evaluate the

reactivity of the corresponding adducts both in TGS settings and in the absence of uPA. Benzotriazole adducts **15a-d** were prepared from benzotriazole and the corresponding aminopyridine and aldehyde compounds (**Scheme 6**) based on a modified reaction protocol from Katritzky *et al.*^[55] The *p*-toluenesulfinic acid adducts **17a-g**, on the other hand, were obtained by reacting *p*-toluenesulfinic acid with the corresponding aminopyridine and aldehyde components (**Scheme 7**). The structure of the imine adducts was confirmed by 2D NMR experiments (HSQC, HMBC). Detailed experimental procedures and characterization data for the preparation of imine adducts **15a-d**, **17a-g** can be found in the Supporting Information (Schemes S4-S5, and the General methods section).

Scheme 6. Synthesis of benzotriazole imine adducts **15a-d**.

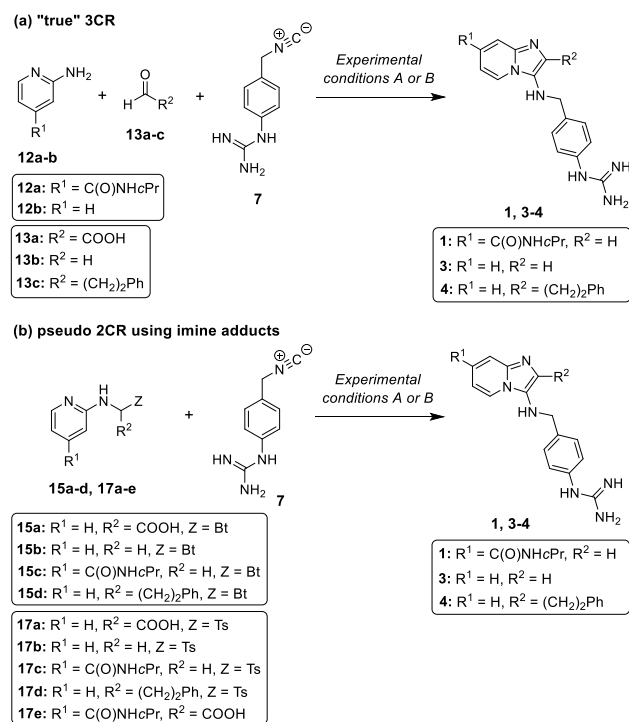


Scheme 7. Synthesis of *p*-toluenesulfinic acid imine adducts **17a-g**.



isocyanide **7** in the absence of enzyme, under both experimental conditions A and B (**Scheme 8**, results summarized in **Tables 2-4**). Yields of a classical GBB protocol (involving condensation of amine, aldehyde and isocyanide **7**) under the same experimental conditions were determined for comparison. The reactivity of adducts that produce reference inhibitor **3** are shown in **Table 2**. Compared to a 'classical' protocol, the use of imine adducts was found to increase product yield under experimental conditions A (**Table 2**, Entries 1-6). Noteworthy, formaldehyde-based adducts perform considerably better than glyoxylate-based analogues. The same trend was observed amongst the non-carboxylated compounds, while performing the reactions under conditions B (**Table 2**, Entries 7-12).

In the second series of experiments, we investigated the formation of inhibitor **1**. First, we compared a 3CR involving glyoxylic acid (**Table 3**, Entry 1) with the reaction of the



Scheme 8. "True" 3CRs and pseudo 2CRs in the absence of uPA towards inhibitors **1**, **3-4**.

p-toluenesulfinic acid adduct **17e** (Entry 2) under experimental conditions A. The benzotriazole analogue of adduct **17e** was not included in this set due its troublesome synthesis. Again, the reaction involving an imine adduct gave higher conversion than the classical 3CR. The same tendency was observed while comparing the 3CR involving formaldehyde (Entry 3) with the reaction of adduct **17c** (Entry 4). However, the reaction with adduct **17c** gave over 3-fold higher conversion than the reaction using the corresponding carboxyl analogue **17e**. The yield of the reaction involving benzotriazole analogue **15c** is not reported here due to its insufficient solubility under the experimental conditions. When these reactions were repeated under the experimental conditions B (Table 3, Entries 5-8), the same reactivity trend was observed.

In the last series of experiments we compared a 3CR forming inhibitor **4** with the corresponding pseudo two-component reactions using imine adducts **15d** and **17d** (Table 4). Reactions performed under conditions A (Entries 1-3) showed that both adducts (**15d**, **17d**) gave comparable conversion to the desired product over time, which was about 2-fold higher than obtained from the 3CR. Under the experimental conditions B (Entries 4-6), the use of imine adduct **17d** again resulted in increased formation of product **4** compared to the classical 3CR.

As a result of their favorable solubility and reactivity, the following on-target experiments were using *p*-toluenesulfinic acid adducts without a carboxylic acid moiety (compounds **17b-d** and **17f-g**).

Table 2. Comparison of 3CRs and pseudo 2CRs towards inhibitor **3** (Scheme 8).

Entry	Imine source	Experimental conditions ^[a]	Yield (cpd. 3) ^[b] [%]
1	12b , 13a	A	0.097
2	15a	A	0.19
3	17a	A	0.16
4	12b , 13b	A	0.51
5	15b	A	0.90
6	17b	A	0.82
7	12b , 13a	B	0.23
8	15a	B	0.30
9	17a	B	0.21
10	12b , 13b	B	0.65
11	15b	B	0.91
12	17b	B	0.77

[a] Experimental conditions. Temperature: rt. **A**: Reaction medium: MES buffer (pH 5.5)/ DMSO (95:5). Reagents concentration: 1 mM. **B**: Reaction medium: HEPES buffer (pH 7.0)/ DMSO (95:5). Reagents concentration: 2.5 mM. [b] Determined by UPLC-TQD-MS measurement and calibration curves, after 24 h reaction time. Average of two experiments.

On-target experiments

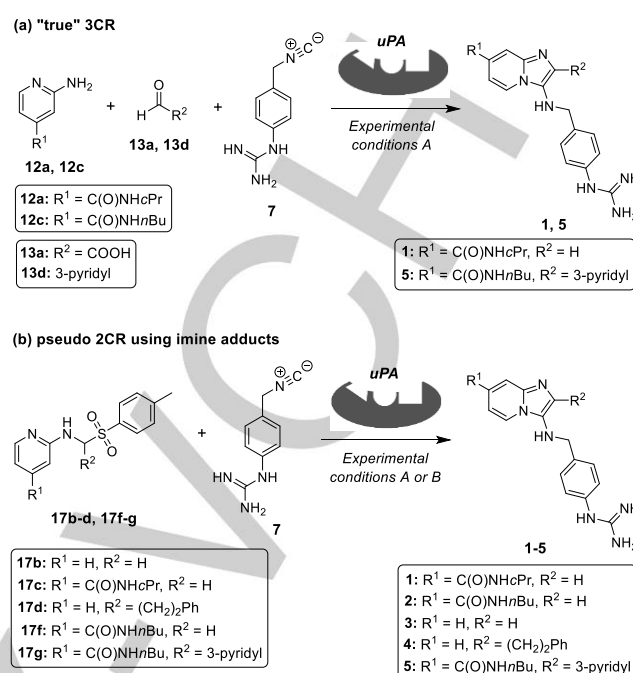
With these optimized conditions in hand, two types of TGS experiments were investigated. A first setup involved a single combination of reactants in the presence of uPA, giving rise to a single inhibitor (Scheme 9). This experimental setup included both (1) "true" 3CRs between separate sets of one aminopyridine, one aldehyde and isocyanide **7** (Scheme 9a), and (2) pseudo 2CRs between separate sets of one imine adduct and isocyanide **7** (Scheme 9b). More specifically, we compared here the outcome of reactions involving five combinations of building blocks leading to uPA inhibitors **1-5**. Within this inhibitor series, relative binding affinities span three orders of magnitude, and we expected the latter to be reflected in the relative rate of the 5 individual enzyme-templated reactions, based on theoretical considerations. A second setup explored in this study, involved a pseudo 2CR featuring the simultaneous introduction of two imine adducts to isocyanide **7**, while other experimental parameters remained constant (Scheme 10). Although the latter experiment starts from the same basic assumptions, it is different from the first one because it includes competition between building blocks demonstrating different binding affinities.

The first on-target experiment involved a "classical" 3CR between 2-aminopyridine **12a**, glyoxylic acid **13a** and isocyanide

Table 3. Comparison of 3CRs and pseudo 2CRs towards inhibitor 1 (Scheme 8).

Entry	Imine source	Experimental conditions ^[a]	Yield (cpd. 1) ^[b] [%]
1	12a, 13a	A	0.12
2	17e	A	0.18
3	12a, 13b	A	0.43
4	17c	A	0.56
5	12a, 13a	B	0.043
6	17e	B	0.12
7	12a, 13b	B	0.15
8	17c	B	0.23

[a] Experimental conditions. Temperature: rt. **A:** Reaction medium: MES buffer (pH 5.5)/ DMSO (95:5). Reagents concentration: 1 mM. **B:** Reaction medium: HEPES buffer (pH 7.0)/ DMSO (95:5). Reagents concentration: 2.5 mM. [b] Determined by UPLC-TQD-MS measurement and calibration curves, after 24 h reaction time. Average of two experiments.

**Scheme 9.** On-target version of the 3CRs and pseudo 2CRs towards uPA inhibitors.**Table 4.** Comparison of 3CRs and pseudo 2CRs towards inhibitor 4 (Scheme 8).

Entry	Imine source	Experimental conditions ^[a]	Yield (cpd. 4) ^[b] [%]
1	12b, 13c	A	0.33
2	15d	A	0.58
3	17d	A	0.61
4	12b, 13c	B	1.3
5	15d	B	YND ^[c]
6	17d	B	2.1

[a] Experimental conditions. Temperature: rt. **A:** Reaction medium: MES buffer (pH 5.5)/ DMSO (95:5). Reagents concentration: 1 mM. **B:** Reaction medium: HEPES buffer (pH 7.0)/ DMSO (95:5). Reagents concentration: 2.5 mM. [b] Determined by UPLC-TQD-MS measurement and calibration curves, after 24 h reaction time. Average of two experiments. [c] Yield of this reaction was not determined (YND) due to insufficient solubility of compound 15d under the experimental conditions.

7 to form imidazopyridine **1**, a uPA inhibitor with nanomolar potency ($IC_{50} = 184 \pm 7$ nM) (Scheme 9a). The later experiment was performed under experimental conditions A, using as

reaction medium MES buffer at pH 5.5 / DMSO (95:5), each of the building blocks at 1 mM concentration, and uPA at 21 μ M concentration. Besides, a negative control reaction in buffer (CTRL) was included here. Subsequently, the on-target reaction as well as the control experiment were monitored over time. As a result, in contrast to our expectations, this 3CR showed almost identical conversion in both the experiment involving uPA and the CTRL (Table 5, Entries 1-2). Moreover, the latter were characterized by very low reaction rates. Here the reaction with uPA resulted after 24 h in 0.13% yield, corresponding to 1.3 μ M of the product **1**.

Therefore, we decided to investigate next the pseudo 2CR reaction variant involving isocyanide **7** and adduct **17c** (Scheme 9b). The later on-target experiment was performed first under experimental conditions A. Additionally, two control experiments were included this time: (1) a negative control reaction in buffer, and (2) a reaction using human serum albumin (HSA) instead of uPA. This experiment again showed that both the reaction involving uPA as well as the CTRL demonstrated very comparable product formation (Table 5, Entries 3-4). However, not unexpectedly, this pseudo 2CR was characterized by an over 5-fold higher conversion than the 3CR reaction variant. In all performed experiments, the pseudo 2CR reaction mainly proceeded during the first 24 h, with the biggest increase in product formation within the first 5 h. After 24 h, the reaction rate was neglectable. For the sake of completeness, experiments were nonetheless monitored for 48 h, and after 1 week. Here, the reaction involving uPA showed the same conversion as the CTRL experiment in the whole timeframe. After 24 h, the reaction resulted in 0.68% yield, what corresponded to 6.8 μ M

Table 5. Results of on-target experiments towards uPA inhibitors **1-2** (Scheme 9).

Entry	Reagents	Product	Target or control	Experimental conditions ^[a]	Yield ^[b] [%]	Relative conc. ^[c]
1	12a, 13a, 7	1	uPA	A, [uPA] = 21 μ M	0.13	1.1
2			buffer	A	0.12	1
3	17c, 7	1	uPA	A, [uPA] = 21 μ M	0.68	1
4			buffer	A	0.68	1
5			HSA	A, [HSA] = 21 μ M	0.61	0.89
6	17c, 7	1	uPA	B, [uPA] = 20.5 μ M	0.20	0.98
7			buffer	B	0.21	1
8			HSA	B, [HSA] = 21 μ M	0.18	0.88
9	17c, 7	1	uPA	B, [uPA] = 84 μ M	0.19	0.84
10			buffer	B	0.22	1
11	17f, 7	2	uPA	A, [uPA] = 21.5 μ M	0.78	1.02
12			buffer	A	0.76	1
13			HSA	A, [HSA] = 21 μ M	0.73	0.95
14	17f, 7	2	uPA	B, [uPA] = 20 μ M	0.23	0.97
15			buffer	B	0.23	1
16			HSA	B, [HSA] = 21 μ M	0.21	0.89

[a] Experimental conditions. Temperature: rt. **A:** Reaction medium: MES buffer (pH 5.5)/ DMSO (95:5). Reagents concentration: 1 mM. **B:** Reaction medium: HEPES buffer (pH 7.0)/ DMSO (95:5). Reagents concentration: 2.5 mM. [b] Determined by UPLC-TQD-MS measurement and calibration curves, after 24 h reaction time. Average of two experiments. [c] Relative concentration refers to the product concentration in the sample calculated relatively to the product concentration in the corresponding negative control in buffer, obtained by division. Within a single on-target experiment, product concentration in the negative control in buffer refers to as 1.

of the product **1**. The control experiment with HSA showed that HSA does not promote product formation, but in fact interferes with the reaction resulting in lower conversion (Table 5, Entry 5).

The pseudo two-component reaction on-target towards inhibitor **1** was then repeated under experimental conditions B, using HEPES buffer at pH 7.0 / DMSO (95:5) as the reaction medium, and each of the building blocks (isocyanide **7** and adduct **17c**) at 2.5 mM concentration. As a result, again, the reaction involving uPA and CTRL showed a very comparable conversion over time, and the control with HSA gave lower conversion (Table 5, Entries 6-8).

Due to the observed lack of difference between the experiment involving uPA and CTRL, we decided to investigate the effect of increased enzyme concentration. Hence, we pursued the on-target experiment with 4-fold higher concentration of uPA (84 μ M) using experimental conditions B. As a result, the on-target experiment showed lower reaction outcome than the corresponding CTRL experiment (Table 5, Entries 9-10). The

possibility of incomplete analyte recovery from solutions containing the highest protein concentrations was also evaluated here, but the recovery was found to be identical for solutions with and without protein (see Supporting Information, Scheme S11, and the General protocol for pseudo two-component (2CR) reactions on-target). We therefore assume that the lower reaction outcome observed in case of experiments involving the highest uPA concentration is due to interference of the enzyme with the reaction. The latter may be a result of e.g. (1) side reactions between enzyme amino acid side chains and reagents or (2) faster decomposition of the imine adduct **17c** or isocyanide compound **7**.

The second pseudo two-component reaction tested on-target, involved isocyanide **7** and adduct **17f**. This reaction affords the most potent uPA-inhibitor within the reference set: compound **2** ($IC_{50} = 97 \pm 10$ nM). The same experimental strategy as described in the previous experiment was applied. First, we reacted isocyanide **7** and adduct **17f** under

Table 6. Results of on-target experiments towards uPA inhibitors **3-5** (Scheme 9).

Entry	Reagents	Product	Target or control	Experimental conditions ^[a]	Yield ^[b] [%]	Relative conc. ^[c]
1	17b, 7	3	uPA	A, [uPA] = 21.5 μ M	0.68	1.07
2			buffer	A	0.63	1
3			HSA	A, [HSA] = 21 μ M	0.64	1.02
4	17b, 7	3	uPA	B, [uPA] = 20 μ M	0.81	0.93
5			buffer	B	0.87	1
6			HSA	B, [HSA] = 21 μ M	0.77	0.88
7	17d, 7	4	uPA	A, [uPA] = 20 μ M	0.46	1.01
8			buffer	A	0.45	1
9	12c, 13d, 7	5	uPA	A, ^[d] [uPA] = 22 μ M	0.0056	0.21
10			buffer	A ^[d]	0.028	1
11			HSA	A, ^[d] [HSA] = 22 μ M	0.025	0.89
12	17g, 7	5	uPA	A, ^[d] [uPA] = 22 μ M	0.0086	0.2
13			buffer	A ^[d]	0.045	1
14			HSA	A, ^[d] [HSA] = 21 μ M	0.042	0.93
15	17g, 7	5	uPA	B, ^[d] [uPA] = 22 μ M	0.013	0.29
16			buffer	B ^[d]	0.045	1
17			HSA	B, ^[d] [HSA] = 22 μ M	0.041	0.91

[a] Experimental conditions. Temperature: rt. **A:** Reaction medium: MES buffer (pH 5.5)/ DMSO (95:5). Reagents concentration: 1 mM. **B:** Reaction medium: HEPES buffer (pH 7.0)/ DMSO (95:5). Reagents concentration: 2.5 mM. [b] Determined by UPLC-TQD-MS measurement and calibration curves, after 24 h reaction time. Average of two experiments. [c] Relative concentration refers to the product concentration in the sample calculated relatively to the product concentration in the corresponding negative control in buffer, obtained by division. Within a single on-target experiment, product concentration in the negative control in buffer refers to as 1. [d] Due to a lower reactivity, this reaction required higher reagent concentration. Experimental conditions **A;** reagents concentration: 2.5 mM. Experimental conditions **B;** reagents concentration: 5 mM.

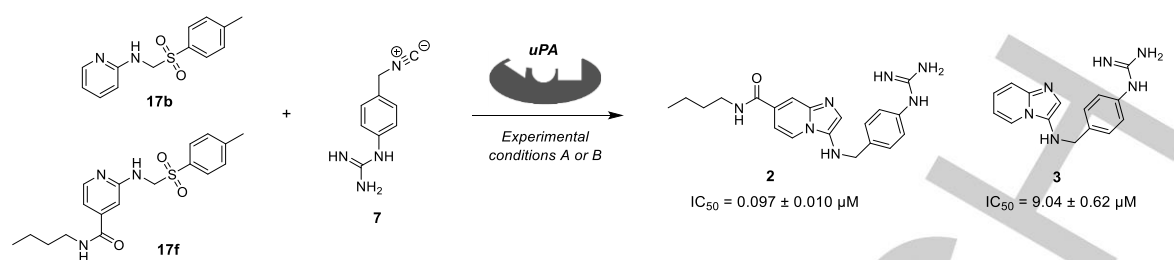
experimental conditions A. Second, the same reaction was repeated under experimental conditions B. However, experiments involving a higher concentration of uPA were not included because of the observed interference of high amounts of enzyme on reaction yield. These experiments gave very comparable results to the on-target reaction for the synthesis of inhibitor **1** (Table 5, Entries 11-16). In particular, neither the experiment in MES buffer nor HEPES buffer demonstrated uPA-templated amplification of compound **2** in the whole timeframe. Also here, control experiments with HSA showed lower reaction outcome.

Next, we compared the outcome of the above experiments (involving highly potent inhibitors **1** and **2**, Table 5), with the outcome of reactions affording the less potent ligands **3-5** (Table 6). We hypothesized that ligands of nanomolar affinity could cause catalyst poisoning, thus inhibiting the enzyme to further

function as template during the on-target process. This situation could be different in reactions affording less potent inhibitors.

To this end, isocyanide **7** was reacted with adduct **17b**, to afford the micromolar inhibitor **3** ($IC_{50} = 9.04 \pm 0.62 \mu$ M). The same experimental strategy was applied as for compound **2**. Again, however, neither the on-target reaction performed under conditions A nor B showed uPA-templated formation of compound **3** over 24 h (Table 6, Entries 1-6) as well as 48 h. The experiment aiming at the on-target synthesis of high-micromolar inhibitor **4** from the adduct **17d** and isocyanide **7** had a similar outcome (Table 6, Entries 7-8).

The next set of experiments was aiming at the uPA-templated synthesis of uPA inhibitor **5** ($IC_{50} = 6.89 \pm 0.80 \mu$ M). First, a 3CR between aminopyridine **12c**, nicotinaldehyde **13d**



Scheme 10. Competition-based experiment using adducts **17b** and **17f** towards inhibitors **2** and **3**.

Table 7. Results of the competition-based experiment towards inhibitors **2** and **3** (Scheme 10).

Entry	Target or control	Experimental conditions ^[a]	Yield (cpd. 2) ^[b] [%]	Rel. conc. ^[c] cpd. 2	Yield (cpd. 3) ^[b] [%]	Rel. conc. ^[c] cpd. 3
1	uPA	A, [uPA] = 21.5 μM	0.92	1.04	0.83	1.01
2	buffer	A	0.89	1	0.82	1
3	HSA	A, [HSA] = 21 μM	0.84	0.94	0.79	0.96
4	uPA	B, [uPA] = 20 μM	0.21	0.97	0.61	0.98
5	buffer	B	0.22	1	0.62	1
6	HSA	B, [HSA] = 21 μM	0.19	0.87	0.53	0.86

[a] Experimental conditions. Temperature: rt. **A:** Reaction medium: MES buffer (pH 5.5)/ DMSO (95:5). Reagents concentration: 1 mM. **B:** Reaction medium: HEPES buffer (pH 7.0)/ DMSO (95:5). Reagents concentration: 2.5 mM. [b] Determined by UPLC-TQD-MS measurement and calibration curves, after 24 h reaction time. Average of two experiments. [c] Relative concentration refers to the product concentration in the sample calculated relatively to the product concentration in the corresponding negative control in buffer, obtained by division. Within a single on-target experiment, product concentration in the negative control in buffer refers to as 1.

and isocyanide **7**, in the presence of uPA was evaluated under experimental conditions A. Due to the observed lower reactivity of the reagents, this reaction required higher reagent concentration. As a result, the reaction with uPA gave over 4 times *lower* conversion than the CTRL. However, the experiment with HSA showed only slightly lower conversion than the CTRL (Table 6, Entries 9-11).

The outcome of the 3CR towards inhibitor **5** was then compared with the corresponding pseudo 2CR on-target. This 2CR involved imine adduct **17g** and isocyanide **7**. Although notably faster, the pseudo 2CR on-target demonstrated the same trend as its 3CR counterpart. More precisely, we observed that both under adapted experimental conditions A and B, the reaction involving uPA demonstrated 3-5 times *lower* outcome than the corresponding CTRL reaction. Furthermore, similar as before, the experiment with HSA showed only slightly lower conversion than the CTRL (Table 6, Entries 12-17).

We do not have a clear explanation why both the classical 3CR and the pseudo 2CR with uPA towards inhibitor **5** result in lower yield than the corresponding control reactions. Certainly, this experiment shows that enzymes may not only promote, but

also interfere with the on-target reaction, what in some cases could complicate the proper interpretation of TGS results. Here, comparing negative control reactions in buffer with the reactions involving uPA, can indeed hint towards interference of the enzyme with the studied reaction. On the other hand, discrepancy in the rates of reactions involving uPA and HSA can be related to differences in amino acid sequence of uPA and HSA reflected by their various isoelectric points ($pI(\text{uPA}) = 8.69$ vs. $pI(\text{HSA}) = 5.8$).^[48, 65]

Next, we designed a competition-based experiment involving two uPA ligands displaying a 100-fold difference in binding affinity: compounds **2** and **3**. The rationale behind this experiment was to investigate the possibility of TGS *via* an alternative strategy than in the foregoing experiments, namely by allowing direct competition between building blocks of different affinity. This competition was expected to lead to a product distribution reflecting the relative binding potencies (represented by their IC_{50} -values) of the inhibitors. In this way, even in cases where the enzyme would slow down the reaction, the relative amounts of the formed products could be an indication of the enzyme-templated reactivity. Likewise, product distribution

should be notably different between the on-target reaction and CTRL, in which products are formed only according to the chemical reactivities of building blocks.

Herein, we reacted the corresponding imine adducts **17b** and **17f** with isocyanide **7** in the presence of uPA under conditions A and B (**Scheme 10**). As a result, the relative amounts of products **2** and **3** formed in this experiment were comparable under each of the applied experimental conditions (A and B), whereas direct competition between building blocks should be reflected by considerably higher amplification of compound **2** over **3**. In addition, the CTRL experiment showed the same product distribution as the reaction involving uPA (**Table 7**). Hence, it can be concluded that this experiment did not show direct competition for uPA's active site between the selected building blocks.

Conclusions

In conclusion, we have described our efforts towards the development of a target-guided version of the GBB reaction. Our study relied on a well-defined model system involving urokinase (uPA) as target protein. A set of imidazopyridine-based inhibitors of uPA, which were previously reported by us, served as reference compounds in this work.^[32] A major hurdle to take when developing an on-target protocol for the GBB reaction, was found to be the imine formation step in aqueous media. Most likely, the latter will represent a general challenge in the development of TGS protocols for medicinally relevant MCRs involving imine intermediates (e.g., the Ugi reaction, Hantzsch synthesis, and A3-reaction). In order to address imine formation problems, we applied a strategy based on trapping imines in the form of a metastable adduct with either benzotriazole or *p*-toluenesulfonic acid. Subsequently, a number of prepared imine adducts were reacted with an isocyanide in the presence of uPA following the developed on-target protocol. Unfortunately, our on-target experiments for the formation of uPA inhibitors **1-5**, did not demonstrate a notable enzyme-templating activity. The latter applied for both the reactions involving a single combination of building blocks, and a competition-based experiment involving two combinations of building blocks. These experimental results were not in line with our initial molecular modeling study, which indicated that the templated GBB reaction is sterically possible in uPA's active site.

This study demonstrates that, in target-guided research, moving from a 2CR to a 3CR is associated with increased experimental complexity. Nonetheless, there might be niches of reactivity within the MCR chemistry that are more amenable to typical experimental conditions of TGS. Finally, the strategy of stabilizing an imine intermediate in the form of a reversible adduct, as described in this report, can be further implemented while developing other MCRs on-target.

Experimental Section

General methods. Commercially sourced reagents were used without further purification. All solvents were reagent-grade, and in case of

purification of the final compounds HPLC grade were used. Where necessary, flash purification was performed with a Biotage ISOLERA One flash system equipped with an internal variable dual-wavelength diode array detector (200-400 nm). SNAP cartridges were used for normal phase purifications KP-Sil and for reversed phase purifications KP-C18-HS. Dry sample loading was done by self-packing samplet cartridges using silica and Celite 545, respectively, for normal and reversed phase purifications. Gradients used varied for each purification. Solvents used for the column chromatography were ethyl acetate, heptane and methanol. ¹H NMR and ¹³C NMR spectra were recorded with a Bruker Avance DRX 400 spectrometer (400 MHz for ¹H, 101 MHz for ¹³C) at 21 °C. Chemical shifts (δ) are reported in ppm relative to the residual solvent peak. Splitting patterns are indicated as singlet (s), doublet (d), triplet (t), quartet (q), multiplet (m), broad (br). The coupling constants (*J*) are reported in hertz (Hz). Melting points were determined with a melting point M-560 apparatus (BUCHI) and are uncorrected. A Waters Acquity UPLC[®] system coupled to a Waters TUV detector and a Waters TQD ESI mass spectrometer was used. The wavelength for UV detection was 254 nm. A Waters Acquity UPLC[®] BEH C18 1.7 μ m, 2.1 mm x 50 mm column was used. Column temperature was 30 °C. Regarding conditions of the mobile phase, monitoring of the reaction progress, as well as product purity determination was performed using Method I. This method used as mobile phase solvent A: water with 0.1% formic acid, and solvent B: acetonitrile with 0.1% formic acid. Conditions of the mobile phase (Method I): flow 0.7 mL/min, gradient of the mobile phase: 0-0.15 min: 95% solvent A, 5% solvent B (isocratic); 0.15-2.5 min: linear gradient from 5% to 100% solvent B; 2.5-3.25 min: 100% solvent B (isocratic); 3.25-4.0 min: further system equilibration (95% solvent A, 5% solvent B), flow 0.35 mL/min.

Target-guided synthesis. Target-guided synthesis experiments were monitored using a Waters Acquity UPLC[®] system and mobile phase conditions described under Method II. The latter method used as mobile phase solvent A: 5 mM ammonium acetate buffer (pH 4.0 adjusted with formic acid); solvent B: acetonitrile. Conditions of the mobile phase (Method II): 0.65 mL/min, gradient of the mobile phase: 0-0.15 min: 98% solvent A, 2% solvent B (isocratic); 0.15-1.5 min: linear gradient from 2% to 20% solvent B; 1.5-1.8 min: linear gradient from 20% to 50% solvent B; 1.8-2.1 min: linear gradient from 50% to 100% solvent B; 2.1-2.2 min: 100% solvent B (isocratic); 2.2-2.6 min: 98% solvent A, 2% solvent B (isocratic); 2.6-3.0 min: further system equilibration (98% solvent A, 2% solvent B). Samples were analyzed using a full scan method and MRM method. MRM methods were based on a tuning file and prepared for each of the investigated products separately. Product quantification was based on calibration curves prepared using reference compounds **1-5**. The calibration curves were prepared by plotting the response measured with UPLC-TQD-MS in the MRM mode against the injected product concentration. The experiments were performed in duplo, and the reported reaction yields are the average of these two experiments. Based on the magnitude of the calculated standard deviation (SD), reporting two significant digits in the reaction yields was considered statistically justified. Data collection and analysis were performed using Waters MassLynx software and Microsoft Excel.

General protocol for TGS via the GBB reaction. In a 0.5 mL Eppendorf tube were combined uPA solution in 0.2 M MES buffer at pH 5.5 (150 μ L), isocyanide **7** solution (10 mM in MES buffer, 20 μ L), aminopyridine compound solution (20 mM in DMSO, 10 μ L), and aldehyde solution (10 mM in MES buffer, 20 μ L). The final concentration of uPA in the reaction mixture was approx. 21 μ M. The resulting mixture was shaken at rt for at least 48 h, and was monitored at time 0 h, 24 h, 48 h, and in case of a limited number of experiments after 1 week. When 0.2 M HEPES buffer of pH 7.0 was used as reaction medium, higher reagent concentrations were used. In this case, the reaction mixture comprised uPA solution in 0.2 M HEPES buffer at pH 7.0 (150 μ L), isocyanide **7** solution (25 mM in HEPES

FULL PAPER

buffer, 20 μ L), aminopyridine compound solution (50 mM in DMSO, 10 μ L), and aldehyde solution (25 mM in HEPES buffer, 20 μ L). Except reagent concentrations, all other experimental conditions were as before.

General protocol for the pseudo two-component reaction on-target.

All imine adduct solutions were freshly prepared prior to use. In a 0.5 mL Eppendorf tube, were combined uPA solution in 0.2 M MES buffer at pH 5.5 (170 μ L), isocyanide **7** solution (10 mM in MES buffer, 20 μ L), and imine adduct solution (20 mM in DMSO, 10 μ L). The final concentration of uPA in the reaction mixture was approx. 21 μ M. The resulting mixture was shaken at rt for 48 h, and was monitored at time 0 h, 24 h, 48 h, and in case of a limited number of experiments after 1 week. When 0.2 M HEPES buffer of pH 7.0 was used as reaction medium, higher reagent concentrations were used. In this case, the reaction mixture comprised uPA solution in 0.2 M HEPES buffer at pH 7.0 (170 μ L), isocyanide **7** solution (25 mM in HEPES buffer, 20 μ L), and imine adduct solution (50 mM in DMSO, 10 μ L). Except reagent concentrations, all other experimental conditions were as before.

General protocol for a competition experiment using a mixture of two imine adducts.

All imine adduct solutions were freshly prepared prior to use. In a 0.5 mL Eppendorf tube, were combined uPA solution in 0.2 M MES buffer at pH 5.5 (170 μ L), isocyanide **7** solution (10 mM in MES buffer, 20 μ L), and a solution containing two imine adducts (20 mM of each adduct in DMSO, 10 μ L). The final concentration of uPA in the reaction mixture was approx. 21 μ M. The resulting mixture was shaken at rt for 48 h, and was monitored at time 0 h, 24 h, 48 h. When 0.2 M HEPES buffer of pH 7.0 was used as reaction medium, higher reagent concentrations were used. In this case, the reaction mixture comprised uPA solution in 0.2 M HEPES buffer at pH 7.0 (170 μ L), isocyanide **7** solution (25 mM in HEPES buffer, 20 μ L), and a solution containing two imine adducts (50 mM of each adduct in DMSO, 10 μ L). Except reagent concentrations, all other experimental conditions were as before.

Molecular Modeling. Molecular modeling was performed with help of suitable software.^[33] Molecular visualization was performed with *Molecular Operating Environment (MOE)*, 2018. Structure preparation of the protein was performed using the system prepare module in MOE. Docking was performed with FRED. Marvin was used for drawing and displaying chemical structures. The crystal structure of uPA was taken from the protein data bank; PDB code: 4MNW.^[34] The enzyme was complexed with the ligand bicyclic peptide UK749.^[35] This ligand was removed prior to docking. The enzyme structure was kept fixed.

Supporting Information (see footnote on the first page of this article). Detailed experimental procedures and characterization data for the preparation of all reported compounds, as well as experimental data concerning TGS experiments.

Acknowledgements

R.G. is thankful to the Research Foundation – Flanders (FWO) for the postdoctoral research grant. This work received support from the University Research Fund (BOF-KP). The Laboratory of Medicinal Chemistry is a partner of the Antwerp Drug Discovery Network (www.addn.be).

Keywords: target-guided synthesis • multicomponent reactions • imine adducts • urokinase • inhibitors

- [1] D. Bosc, J. Jakhlal, B. Deprez, R. Deprez-Poulain, *Future Med. Chem.* **2016**, *8*, 381-404.
- [2] M. Jaegle, E. L. Wong, C. Tauber, E. Nawrotzky, C. Arkona, J. Rademann, *Angew. Chem. Int. Ed.* **2017**, *56*, 7358-7378.
- [3] E. Oueis, C. Sabot, P.-Y. Renard, *Chem. Commun.* **2015**, *51*, 12158-12169.
- [4] M. Mondal, A. K. Hirsch, *Chem. Soc. Rev.* **2015**, *44*, 2455-2488.
- [5] K. B. Sharpless, R. Manetsch, *Expert Opin. Drug Discov.* **2006**, *1*, 525-538.
- [6] M. Whiting, J. Muldoon, Y.-C. Lin, S. M. Silverman, W. Lindstrom, A. J. Olson, H. C. Kolb, M. G. Finn, K. B. Sharpless, J. H. Elder, V. V. Fokin, *Angew. Chem. Int. Ed.* **2006**, *45*, 1435-1439.
- [7] W. G. Lewis, L. G. Green, F. Grynszpan, Z. Radić, P. R. Carlier, P. Taylor, M. G. Finn, K. B. Sharpless, *Angew. Chem. Int. Ed.* **2002**, *41*, 1053-1057.
- [8] J. D. Cheeseman, A. D. Corbett, J. L. Gleason, R. J. Kazlauskas, *Chem. Eur. J.* **2005**, *11*, 1708-1716.
- [9] A. Krasinski, Z. Radić, R. Manetsch, J. Raushel, P. Taylor, K. B. Sharpless, H. C. Kolb, *J. Am. Chem. Soc.* **2005**, *127*, 6686-6692.
- [10] R. Deprez-Poulain, N. Hennuyer, D. Bosc, W. G. Liang, E. Enée, X. Marechal, J. Charton, J. Totobenazara, G. Berte, J. Jakhlal, T. Verdelet, J. Dumont, S. Dassonneville, E. Woitrain, M. Gauriot, C. Paquet, I. Duplan, P. Hermant, F.-X. Cantrelle, E. Sevin, M. Culot, V. Landry, A. Herledan, C. Piveteau, G. Lippens, F. Leroux, W.-J. Tang, P. van Endert, B. Staels, B. Deprez, *Nat. Commun.* **2015**, *6*, 8250.
- [11] X. Hu, J. Sun, H. G. Wang, R. Manetsch, *J. Am. Chem. Soc.* **2008**, *130*, 13820-13821.
- [12] S. S. Kulkarni, X. Hu, D. Kenichiro, H.-G. Wang, R. Manetsch, *ACS Chem. Biol.* **2011**, *6*, 724-732.
- [13] M. Jaegle, T. Steinmetzer, J. Rademann, *Angew. Chem. Int. Ed. Engl.* **2017**, *56*, 3718-3722.
- [14] R. Nguyen, I. Huc, *Angew. Chem. Int. Ed.* **2001**, *40*, 1774-1776.
- [15] T. Maki, A. Kawamura, N. Kato, J. Ohkanda, *Protein. Mol. BioSyst.* **2013**, *9*, 940-943.
- [16] F. E. Kwarcinski, M. E. Steffey, C. C. Fox, M. B. Soellner, *ACS Med. Chem. Lett.* **2015**, *6*, 898-901.
- [17] E. Oueis, F. Nachon, C. Sabot, P.-Y. Renard, *Chem. Commun.* **2014**, *50*, 2043-2045.
- [18] R. Manetsch, A. Krasinski, Z. Radić, J. Raushel, P. Taylor, K. B. Sharpless, H. C. Kolb, *J. Am. Chem. Soc.* **2004**, *126*, 12809-12818.
- [19] V. P. Mocharla, B. Colasson, L. V. Lee, S. Röper, K. B. Sharpless, C. H. Wong, H. C. Kolb, *Angew. Chem.* **2005**, *117*, 118-122.
- [20] W. Tieu, T. P. Soares da Costa, M. Y. Yap, K. L. Keeling, M. C. J. Wilce, J. C. Wallace, G. W. Booker, S. W. Polyak, A. D. Abell, *Chem. Sci.* **2013**, *4*, 3533-3537.
- [21] V. P. Mocharla, J. C. Walsh, H. C. Padgett, H. Su, B. Fueger, W. A. Weber, J. Czernin, H. C. Kolb, *ChemMedChem* **2013**, *8*, 43-48.
- [22] A. Dömling, W. Wang, K. Wang, *Chem. Rev.* **2012**, *112*, 3083-3135.
- [23] L. Weber, *Drug Discov. Today Technol.* **2004**, *1*, 261-267.
- [24] E. L. Wong, E. Nawrotzky, C. Arkona, B. G. Kim, S. Beligny, X. Wang, S. Wagner, M. Lisurek, D. Carstjan, J. Rademann, *Nat. Commun.* **2019**, *10*, 66.
- [25] N. Devi, R. K. Rawal, V. Singh, *Tetrahedron* **2015**, *71*, 183-232.
- [26] K. Groebke, L. Weber, F. Mehlin, *Synlett* **1998**, 661-663.
- [27] C. Blackburn, B. Guan, P. Fleming, K. Shiosaki, S. Tsai, *Tetrahedron Lett.* **1998**, *39*, 3635-3638.
- [28] H. Bienaymé, K. Bouzid, *Angew. Chem. Int. Ed.* **1998**, *37*, 2234-2237.
- [29] K. Dass, A. Ahmad, A. S. Azmi, S. H. Sarkar, F. H. Sarkar, *Cancer Treat. Rev.* **2008**, *34*, 122-136.
- [30] A. H. Mekawy, M. H. Pourgholami, D. L. Morris, *Med. Res. Rev.* **2014**, *34*, 918-956.
- [31] S. Ulisse, E. Baldini, S. Sorrenti, M. D'Armiento, *Curr. Cancer Drug Targets* **2009**, *9*, 32-71.
- [32] R. Gladysz, Y. Adriaenssens, H. De Winter, J. Joossens, A.-M. Lambeir, K. Augustyns, P. Van der Veken, *J. Med. Chem.* **2015**, *58*, 9238-9257.

- [33] Software used: (a) *Molecular Operating Environment (MOE)*, 2018; Chemical Computing Group ULC, 1010 Sherbooke St. West, Suite #910, Montreal, QC, Canada, H3A 2R7, 2018. (b) *FRED*; M. McGann, *J. Chem. Inf. Model.* **2011**, *51*, 578-596. (c) *Marvin*; Marvin 15.10.26, ChemAxon; <http://www.chemaxon.com> (accessed January 10, 2019).
- [34] Crystal structure of uPA: PDB accession code 4MNV; <https://www.rcsb.org/structure/4mnw> (accessed January 31, 2019).
- [35] S. Chen, D. Bertoldo, A. Angelini, F. Pojer, C. Heinis, *Angew. Chem. Int. Ed. Engl.* **2014**, *53*, 1602-1606.
- [36] A. R. Griswold, P. Cifani, S. D. Rao, A. J. Axelrod, M. M. Miele, R. C. Hendrickson, A. Kentsis, D. A. Bachovchin, *Cell Chem. Biol.* **2019**, *26*, 1-7.
- [37] H. Stöckmann, A. A. Neves, S. Stairs, K. M. Brindle, F. J. Leeper, *Org. Biomol. Chem.* **2011**, *9*, 7303-7305.
- [38] H. M. Walborsky, G. E. Niznik, *J. Org. Chem.* **1972**, *37*, 187.
- [39] Actosolv® (urokinase 600 000 IU, powder for solution for injection), Eumedica Pharmaceuticals. Enzyme purification was performed using a desalting column PD MiniTrap™ G-25, GE Healthcare.
- [40] M. C. Pirrung, K. Das Sarma, *J. Am. Chem. Soc.* **2004**, *126*, 444-445.
- [41] A. Dömling, *Chem. Rev.* **2006**, *106*, 17-89.
- [42] S. Marcaccini, T. Torroba, *Nature Protocols*, **2007**, *2*, 632-639.
- [43] Y. Yabushita, *Biotechnol. Appl. Biochem.* **1988**, *10*, 294-300.
- [44] J. B. Moffat, *Catalysis Reviews: Science and Engineering*, **1978**, *18*, 199-258.
- [45] G. A. Souza, M. M. M. Peixoto, A. P. F. Santos, W. J. Baader, *ChemistrySelect* **2016**, *1*, 2307-2315.
- [46] Y. Shimada, S. Kondo, Y. Ohara, K. Matsumoto, T. Katsuki, *SYNLETT* **2007**, *15*, 2445-2447.
- [47] N. E. Good, G. D. Winget, W. Winter, T. N. Connolly, S. Izawa, R. M. Singh, *Biochemistry* **1966**, *5*, 467-477.
- [48] ExpASy ProtParam tool; <https://web.expasy.org/protparam/>; provided sequence: mature human urokinase (accessed January 30, 2019)
- [49] L. Di, E. H. Kerns, *Drug Discov. Today* **2006**, *11*, 446-451.
- [50] C. Peruzzotti, S. Borrelli, M. Ventura, R. Pantano, G. Fumagalli, M. S. Christodoulou, D. Monticelli, M. Luzzani, A. L. Fallacara, C. Tintori, M. Botta, D. Passarella, *ACS Med. Chem. Lett.* **2013**, *4*, 274-277.
- [51] K. K. Murray, R. K. Boyd, M. N. Eberlin, G. J. Langley, L. Li, Y. Naito, *Pure Appl. Chem.*, **2013**, *85*, 1515-1609.
- [52] M. Mondal, M. Y. Unver, A. Pal, M. Bakker, S. P. Berrier, A. K. H. Hirsch, *Chem. Eur. J.* **2016**, *22*, 14826-14830.
- [53] A. K. Yocum, A. M. Chinnaiyan, *Brief Funct. Genomic. Proteomic.* **2009**, *8*, 145-157.
- [54] J. J. Maury, D. Ng, X. Bi, M. Bardor, A. B. Choo, *Anal Chem.* **2014**, *86*, 395-402.
- [55] A. R. Katritzky, L. Urogdi, *J. Chem. Soc., Perkin Trans. 1*, **1990**, *0*, 1853-1857.
- [56] A. R. Katritzky, M. Sutharchanadevi, L. Urogdi, *J. Chem. Soc., Perkin Trans. 1*, **1990**, *0*, 1847-1851.
- [57] A. R. Katritzky, B. Pilarski, L. Urogdi, *Organic Preparations and Procedures Int.*, **1989**, *21*, 135-139.
- [58] A. R. Katritzky, S. Rachwal, B. Rachwal, *J. Chem. Soc., Perkin Trans. 1*, **1987**, *0*, 799-804.
- [59] H.-J. Grumbach, B. Merla, N. Risch, *Synthesis* **1999**, 1027-1033.
- [60] J.-L. Moutou, M. Schmitt, V. Collot, J.-J. Bourguignon, *Tetrahedron Letters* **1996**, *37*, 1787-1790.
- [61] F. Yang, W. An, Z. Qian, T. Yu, Y. Du, L. Ma, X. Wang, T. Meng, J. Shen, *RSC Adv.* **2015**, *5*, 32015-32019.
- [62] R. Reingruber, T. Baumann, S. Dahmen, S. Bräse, *Adv. Synth. Catal.* **2009**, *351*, 1019-1024.
- [63] M. Petrini, *Chem. Rev.*, **2005**, *105*, 3949-3977.
- [64] W. Li, Y. Lam, *J. Comb. Chem.* **2005**, *7*, 721-725.
- [65] M. Dockal, D. C. Carter, F. Rüker, *J. Biol. Chem.*, **1999**, *274*, 29303-29310.

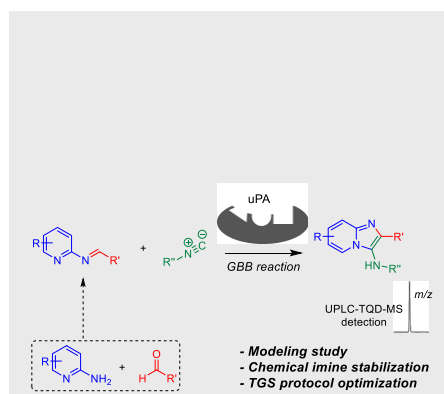
FULL PAPER

Entry for the Table of Contents (Please choose one layout)

Layout 1:

FULL PAPER

While TGS examples generally involve 2CRs, we selected the Groebke-Blackburn-Bienaymé reaction as model 3CR towards urokinase inhibitors. Multiple experimental parameters were optimized. Additionally, chemical imine stabilization strategies were explored. Since imines are also crucial intermediates of other MCRs, this work intends to be a reference for future multicomponent-based TGS studies.



Rafaela Gladysz, Johannes Vrijdag,
Dries Van Rompaey, Anne-Marie
Lambeir, Koen Augustyns, Hans De
Winter, Pieter Van der Veken*

Page No. – Page No.

**Efforts towards an on-target version
of the Groebke-Blackburn-Bienaymé
(GBB) reaction for discovery of
druglike urokinase (uPA) inhibitors**

Layout 2:

FULL PAPER

((Insert TOC Graphic here; max. width: 11.5 cm; max. height: 2.5 cm))

Author(s), Corresponding Author(s)*

Page No. – Page No.

Title

Text for Table of Contents